

## Screening of Inhibition of Calcium Naphthenate Deposition in Crude Oil

Sébastien SIMON\*, Kim EHRET, Pauline DARCEL, Johan SJÖBLOM

Ugelstad Laboratory, Department of Chemical Engineering, the Norwegian University of Science and Technology (NTNU), N-7491 Trondheim, Norway

Nicolas PASSADE-BOUPAT

TOTAL S.A., PERL - Pôle D'Etudes et de Recherche de Lacq, 64170 Lacq, France

Thierry PALERMO

TOTAL S.A., CSTJF - Centre Scientifique et Technique Jean Féger, 64018 Pau, France

### Abstract

One of the initial steps in calcium naphthenate deposition is the reaction between ARN and  $\text{Ca}^{2+}$  leading to the formation of an interfacial gel. After growing, this gel will form calcium naphthenate deposits that are a treat for irregularities in crude oil production and processing. It has previously been shown that crude oil components such as asphaltenes and naphthenic acids can weaken and inhibit the formation of the interfacial gel. Based on this observation, the inhibition efficiency of 4 crude oils are compared. The variations of interfacial tension and interfacial dilational modulus  $E'$  of ARN solution (concentration=10  $\mu\text{M}$ ) in contact with  $\text{Ca}^{2+}$  containing aqueous solution (pH=8) with varying crude oil concentration allows to define a parameter characterizing the interfacial gel inhibition efficiency of crude oils to compare systems with each other. The determined inhibition efficiency order of crude oils is not directly related to the total asphaltene and naphthenic acid contents in the crude oils and therefore cannot be directly predicted by performing simple chemical analysis of the oils. By selectively removing asphaltenes and/or naphthenic acids, it was found that naphthenic acids are the most prevalent inhibitors followed by asphaltenes in the tested crude oils. Other compounds present on crude oil have also a weak inhibition activity on the ARN/ $\text{Ca}^{2+}$  interfacial gel.

Finally, bottle tests were performed to try to upscale results obtained at interfacial scale. Bottle tests were performed at an ARN concentration 10 times higher than for IFT and interfacial rheology measurements. The tests indicate the presence of soft solid material formed by reaction between ARN and  $\text{Ca}^{2+}$  even in the presence of the crude oil that was found to have the highest interfacial gel inhibition efficiency. This apparent contradiction is for moment not understood and means that a better understanding of the ARN/ $\text{Ca}^{2+}$  system is required to be able to extrapolate the results obtained at the interface to bigger scales.

*Keywords:*

Tetrameric acids; ARN; calcium naphthenate deposits; interfacial dilational rheology, crude oil, inhibition

\* Corresponding author. Tel.: (+47) 73 59 16 57      Fax: (+47) 73 59 40 80

E-mail address: [sebastien.simon@chemeng.ntnu.no](mailto:sebastien.simon@chemeng.ntnu.no)

# 1 Introduction

ARN tetrameric acid<sup>a</sup> is responsible for the formation of calcium naphthenate deposit<sup>1,2</sup>, a major treat in crude oil processing. ARN is a family of cycloaliphatic compounds composed of 80 carbon atoms organized as 4 side-chains with carboxylic acid functions at each of their 4 tips<sup>3,4,5,6</sup>. Their structure is very different from other naphthenic acids present in crude oils which are predominantly monoacids<sup>7,8,9</sup>. Since its discovery in 2004<sup>6,10</sup> and the recognition that its presence is a prerequisite for calcium naphthenate deposition, ARN tetrameric acid has been the subject of various research works which can roughly be classified into 2 categories:

-First, several methods have been developed to determine the presence and the concentration of ARN tetrameric acid in petroleum crude oil. The knowledge of the concentration is the first assessment of potential calcium naphthenate deposition risk. As ARN concentration, if even present, is low i.e. in the ppm level<sup>11,12</sup>, this has been challenging. Most of the developed methods used mass spectrometry techniques<sup>13,14,15,16</sup> but a few rely on HPLC with UV detection<sup>11,17</sup>.

-Other studies have focused on the determination of the bulk and interfacial properties of ARN tetrameric acid and their interactions with other crude oil components in order to elucidate the calcium naphthenate deposition mechanism. The knowledge of the mechanism should hopefully allow to be able to predict deposition in newly developed fields<sup>18,19,20</sup>.

Recently, based on previous works and analysis by Vindstad et al.<sup>21</sup>, Broccard et al.<sup>22,23</sup>, and Sjöblom et al.<sup>24,25,26</sup>, Simon et al.<sup>27</sup> have proposed the following calcium deposition mechanism. Initially, due to the depressurization of crude oil during oil production, carbon dioxide is released and, as a consequence, the pH of the produced water is increased. If this increase is high enough, carboxylic acid groups from ARN are ionized and they adsorb at the oil-water interface and reacts with  $\text{Ca}^{2+}$  to form an interfacial gel. This gel grows with time and allows accumulation of material at the interface due to the constant flow of oil bringing new ARN molecules and/or coalescence of droplets that would reduce the interface area without desorption of ARN molecules already present at interface. This gel will eventually form a deposit due to its growth and entrapment of other materials such as particles.

This mechanism is particularly consistent with the interfacial shear<sup>28,29,30</sup> and dilational<sup>27,31,32</sup> rheology measurements performed on model systems i.e. ARN (or its model compound named BP-10) dissolved in organic solvent in presence of an aqueous phase containing  $\text{Ca}^{2+}$  at basic pH. The proposed mechanism is far from being complete. In particular, it does not explain the effect of other crude oil components on the deposition mechanism, especially the interactions between ARN and other crude oil components. Such interactions should have an important role. Indeed, it has been shown that asphaltenes and naphthenic acids are able to inhibit the formation of the interfacial gel. Asphaltenes also seem to be able to desorb and/or disperse already formed ARN/ $\text{Ca}^{2+}$  interfacial gel.

In previous studies<sup>27,32</sup>, we have studied the formation mechanism and the growth of ARN/ $\text{Ca}^{2+}$  interfacial gel as well as the influence of asphaltenes. This new study aims to go further by considering

---

<sup>a</sup>: The name ARN was given to this family of molecules by its discoverer Baugh et al.<sup>6</sup>. It is not an abbreviation and it means “eagle” in old Norwegian.

the influence of whole crude oils on this interfacial gel. This influence will mainly be studied by interfacial dilational rheology, but some attempts will be done to determine how conclusions drawn at the interface could be upscaled using bottle testing.

## 2 Experimental Section

### 2.1 Chemicals

As in our previous studies<sup>27, 32</sup>, ARN samples have been extracted from a calcium naphthenate deposit using the acid-IER (ion exchange resin) method<sup>33</sup>. The obtained sample has been characterized by <sup>1</sup>H NMR<sup>17</sup>.

The crude oils were provided by Total. They are named B, D, E, and U. The results of their characterization are presented in the result section.

Selective removal of asphaltenes and/or naphthenic acids from crude oils allowed to test the influence of these compounds on ARN/Ca<sup>2+</sup> gel formation. The following procedures to remove these compounds were implemented:

-Asphaltenes: 320 mL of n-hexane are added to 8 g of crude oil and the solution is stirred overnight at room temperature. The solution is then filtered on a 0.45 µm HVLP filter (Millipore) and washed with warm n-hexane. This procedure is repeated several times to produce enough materials and the recovered maltene solutions are concentrated with a rotary evaporator before being dried on a block heater at 40°C under a nitrogen flow until the mass is approximately constant and the recovered mass is lower than the initial crude oil mass.

-Naphthenic acids<sup>17</sup>: A glass column was filled with 10.13 g of an anion exchange resin (Biotage Isolete SAX, exchange capacity: 0.75 meq/g) used as the sorbent and conditioned with 250 mL of a 0.1M NaHCO<sub>3</sub> + 0.1M Na<sub>2</sub>CO<sub>3</sub> solution. Afterwards, the column was washed with 200 ml of deionized water to eliminate the excess of counterions, followed by 100 ml of methanol and 400 mL of CH<sub>2</sub>Cl<sub>2</sub>. The amount of crude oil corresponding to 1520 µmol of acid functions diluted with 290mL of CH<sub>2</sub>Cl<sub>2</sub> was loaded into the column and then eluted followed by 300 mL of CH<sub>2</sub>Cl<sub>2</sub>. The deacidified oil fraction was recovered by evaporating the solvent, first with at a rotary evaporator then in a block heater under nitrogen flow and at temperatures up to 47.5°C until the recovered mass is lower than the initial crude oil mass.

The prepared samples are characterized and presented in section 3.1.3.

The other chemicals used in the study are the followings: toluene (99.8 %), benzoic acid (≥ 99.5 %), sodium tetraborate decahydrate-borax (≥99.5%) and sodium bicarbonate (99.5-100.5 %) were obtained from Sigma-Aldrich, tetra-n-butylammonium hydroxide solution 0.1 M, and sodium chloride (for analysis) were from Merck, isopropanol (98 %) and calcium chloride dihydrate (≥99%) were from Sigma, Xylene (mixture of isomers, ≥ 98.5%), n-hexane (for HPLC quality analysis), methanol (100 %),

dichloromethane (99.8 %), and sodium carbonate (99.9 %) were obtained from VWR. Water was from a Milli-Q system from Millipore.

## 2.2 Solution Preparations

The aqueous solutions used in the interfacial study were composed of 20 mM NaCl, 10 mM borax, and 10 mM CaCl<sub>2</sub> and their pH was adjusted to 8 by adding 1 M HCl before introduction of CaCl<sub>2</sub>. Similar aqueous solutions, except the borax content that was increased to 20 mM, were used for the bottle tests.

500  $\mu$ M ARN stock solutions were prepared by dissolving solid ARN in xylene. Solutions were then filtered with 0.2  $\mu$ M PTFE filter.

The solutions for interfacial measurements were prepared by mixing the 500  $\mu$ M filtered ARN solution, pure xylene and pure crude oil (or 1 wt. % crude oil solution in xylene to prepare solution containing less than 0.1 wt. %) to obtain solutions containing 10  $\mu$ M of ARN and variables concentrations of crude oils.

The oil solutions for bottle tests were prepared by mixing the 500  $\mu$ M filtered ARN solution, pure xylene, and pure crude oil to obtain solutions containing 100  $\mu$ M of ARN and volume fractions of crude oil of 0, 0.05, 0.1, 0.15, 0.2, 0.3, 0.4, and 0.5.

For both interfacial measurements and bottle tests, oil solutions that did not contain ARN were prepared to be used as references.

## 2.3 Interfacial Tension and Interfacial Dilational Rheology Measurements.

Interfacial tension and interfacial rheology measurements were carried out following previously published procedures<sup>31</sup>. These experiments were performed with a sessile/pendant drop tensiometer (PAT 1 m) from SINTERFACE Technologies (Berlin, Germany). A 15  $\mu$ L oil drop was created at the tip of a hook in a cuvette filled with 20 mL of aqueous phase. Then IFT was determined for 1 hour to follow up adsorption kinetic. Finally, the volume of the drop was oscillated to determine the E' and E'' moduli (interfacial dilational rheology). The procedure consists of applying five cycles of five different periods (100, 80, 60, 40, and 20 s) at a volume amplitude of 3.5% (for systems containing ARN), and 3.5 or 7 % for other systems. Only the results obtained at a period of 20 s were reported.

Densities of solutions required to calculate IFT values were measured with an Anton Paar DMA 5000M. It was checked that the pH values of the aqueous phases have not changed significantly during measurements. Two parallels were performed for every system studied. The error bars represent the range of obtained experimental values.

## 2.4 Bottle Tests

Bottle tests were performed by introducing 10 mL of the aqueous phase and 10 mL of the xylene solution into glass tubes. Then the tubes were shaken overnight. The following day, the mixtures were

transferred into plastic centrifuge tubes and centrifuged at 7500 rpm for 5 minutes. Aliquots from the interfaces or from “pellets” visible on the centrifuge tube wall were recovered with a pipette or a spatula and transferred on a microscope slide. After taking pictures of the recovered samples with a camera, samples were observed with a Nikon Eclipse ME600 microscope fitted with a CoolSNAP-Pro camera by Media Cybernetics. The pH of the aqueous phases measured after centrifugation shows a slight decrease when the crude oil volume fraction increases, the minimum measured pH being 7.85.

### 3 Results

The result section is divided into two parts. The first one presents the study performed at the oil/water interface from interfacial tension and interfacial dilational rheology measurements. Then, bottle testings are performed in an attempt to upscale results and conclusions obtained at the interface scale.

Four crude oils were used in the study. Their densities, asphaltene contents and total acid numbers (TAN) have been determined and are summarized in table 1. It must be noticed that these crude oils present a large range of properties and chemical compositions with densities varying from 0.873 to 0.950 g/cm<sup>3</sup>, TAN going from 0.32 to 2.85 mg/g, and asphaltene contents ranging from 0.08 to 5.5 wt. %

Crude oil	Density at 25°C (g/cm <sup>3</sup> )	Asphaltenes iC <sub>6</sub> (wt. %)	TAN (mg <sub>KOH</sub> /g <sub>crudeoil</sub> )
B	0.9504 ± 0.0003	5.5 ± 0.2	2.85 ± 0.02
D	0.9193 ± 0.0001	1.57 ± 0.08	1.96 ± 0.01
E	0.9050 ± 0.0001	0.33 ± 0.01	0.32 ± 0.01
U	0.8727 ± 0.0001	0.08 ± 0.06	1.41 ± 0.01

**Table 1:** Characteristics of the crude oils considered in the article. Densities have been measured with an Anton Paar DMA 5000M. Asphaltenes have been precipitated in n-hexane according to the procedure by Hannisdal et al.<sup>34</sup>. The TAN values were determined according to the D664-95 ASTM method. The densities and TAN values are the average of 2 measurements and the error bars represent the range of obtained experimental values. The asphaltene contents are the average of 3 to 5 measurements and the error bars are the standard deviations of the measurements.

#### 3.1 Interfacial Properties

##### 3.1.1 Adsorption kinetics. Influence of Presence of ARN

Figure 1.a presents the variation of the interfacial tension with time for systems composed of crude oil D dissolved at various concentrations in xylene in presence of aqueous phase containing Ca<sup>2+</sup>

and at basic pH. These variations allow to obtain information on the kinetic of adsorption of surface-active components at liquid/liquid interface. In the case of crude oil, these surface-active components are typically asphaltenes, resins, and naphthenic acids<sup>35, 36, 37</sup>. The IFT variations with time are typical of adsorption of surface-active components with a decrease of IFT followed by a plateau<sup>38, 39</sup>. The time to reach the plateau also decreases with crude oil concentration. Finally, IFT classically decreases when the crude oil concentration increases.

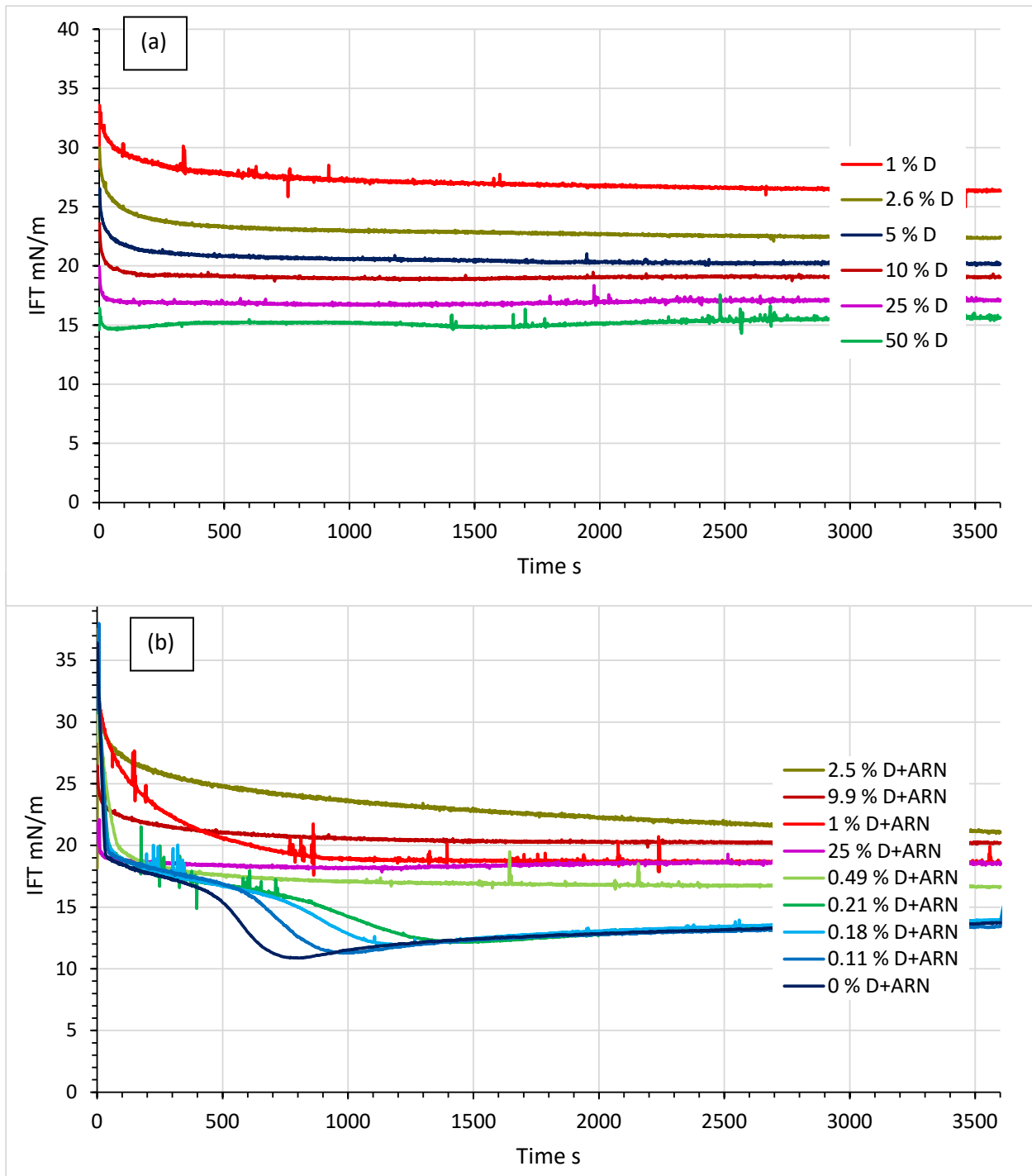


**Figure 1:** Variations of the IFT with time for crude oil D at various concentrations in xylene in absence (a) or in presence (b) of 10  $\mu$ M of ARN. The crude oil concentrations are in weight wt %. The legends in the plots follow the order of the IFT values



The IFT variations with time are completely modified when 10  $\mu\text{M}$  of ARN are added to the oil phase (figure 1.b). In these systems, several behaviors can be identified as a function of the crude oil concentration.

When no crude oil is present and only ARN adsorbs at interface, the IFT sharply decreases first at short times (a few tens of seconds) before decreasing more steadily and reaches a minimum. Then IFT steadily increases reaching a value around 13-14 mN/m after 1 hour. These atypical variations have already been observed on the same system<sup>31</sup> and are attributed to the adsorption of ARN at the oil/water interface, the ionization of the ARN's carboxylic acid functions into carboxylate and their interactions with  $\text{Ca}^{2+}$  resulting in the formation of an interfacial gel. This mechanism is consistent with the  $E'$  values presented in section 3.1.2. Concerning specifically the minimum in IFT variations with time, it is generally attributed for "non-gelling" surfactants to their partition between the oil and water phases that would modify the bulk concentration<sup>40</sup>. However, in the case of figure 1.b, the minimum would rather be more consistent with some reorganization of the ARN/ $\text{Ca}^{2+}$  at the interface with time.

At low crude oil concentrations (up to 0.21 wt. %), the IFT variations have a similar shape. However, the position of the minimum is moved towards longer times. This behavior is attributed to the adsorption of crude oil components in the interfacial layer but still in minor amount compared to systems without crude oil.

From crude oil concentration of 0.5 wt. % up to 2.5 wt. %, the IFT variations with time are more and more reminiscent of systems containing only crude oil components and presented in figure 1.a. Moreover, The IFT measured after 1 hour of adsorption increases with the crude oil concentration. This means that the interfacial energy increases when more crude oil is present. This situation has already been observed and commented in the case of the competitive adsorption between ARN and asphaltenes<sup>32</sup>. Crude oil surface active components become more and more preponderant at interface in detriment to ARN.

Finally, for highest crude oil concentrations, the IFT of systems containing only crude oil or crude oil + ARN becomes similar (figure 2 in the following section). Crude oil surface actives are preponderant at the interface and prevent most of the adsorption of ARN<sup>29, 31</sup>.

The behavior observed in figures 1.a and 1.b are qualitatively similar for the three other crude oils (B, E, and U) but not quantitatively as it will be shown in the next section.

### 3.1.2 Influence of Crude Oil Concentration and Crude Oil Origin

The same type of study as presented in section 3.1.1 has been performed with the 3 other crude oils considered in this study. In order to summarize all the behaviour observed, only the IFT measured after 1 hour of adsorption are reported for all the investigated systems in figure 2. The behaviours observed for the 4 crude oil systems are qualitatively similar.

Indeed, in absence of ARN the IFT gradually decreases when the crude oil concentration increases. It must be noticed that crude oil D, E, and U displays similar IFT values while B crude oil is significantly more surface active. This higher surface activity could be related to the highest contents in surface active components (asphaltenes and naphthenic acids, see table 1) in this crude oil. In presence

of ARN, the IFT is constant at around 13-14 mN/m at low crude oil concentration then increases before approximately levelling off and having variations parallel to the systems without ARN.

In order to explain the IFT variations, interfacial dilational rheology measurements have been performed on all the systems. Figure 3 presents the variations of  $E'$  measured at a period of 20 s. The  $E''$  values are systematically lower than  $E'$  and are not presented. In absence of any crude oil, the  $E'$  value is really high at level around 130 mN/m. This value, consistent with the literature<sup>31</sup>, has been attributed to the formation of an interfacial gel between ionized ARN molecules and  $\text{Ca}^{2+}$ . This value decreases when crude oil is present in the oil phase until reaching low levels (less than 20 mN/m) and still remains higher than  $E''$ . This is characteristic of systems which do not contain ARN and therefore cannot form ARN/ $\text{Ca}^{2+}$  interfacial gel. However, it must be pointed out that these values do not preclude the existence of other types of interfacial structures. For instance, Bouriat et al.<sup>41, 42</sup> have shown the formation of gel-like structure due to the presence of asphaltenes at interface for similar values of  $E'$  ( $\approx 20$  mN/m) by measuring moduli as a function of frequency.

By combining IFT values presented in figure 2 and  $E'$  values from figure 3, a picture of the influence of crude oil on the ARN/ $\text{Ca}^{2+}$  interfacial gel can be drawn. In absence of crude oil an interfacial gel is created as revealed by the high  $E'$  value. Then indigenous crude oil surfactants adsorb at interface weakening the ARN/ $\text{Ca}^{2+}$  interfacial gel ( $E'$  value decreases and IFT increases). Finally, at higher crude oil concentration, the crude oil dominates the composition and prevent the formation of an interfacial gel due to the tetrameric acid (low  $E'$  value, IFT close to the values obtained in absence of ARN).

Even if the 4 crude oils have similar qualitative behaviour in presence of ARN, quantitatively there are significant differences especially at low crude oil concentrations as shown in figure 4 which specifically compares  $E'$  moduli for all the crude oil+ARN systems up to 1 % crude oil concentration. This figure shows that the amount of crude oil necessary to reduce  $E'$  value, and therefore inhibit the formation of ARN/ $\text{Ca}^{2+}$  gel depends on the crude oil. The order is the following: very small amounts of crude oils U and B are required to inhibit the formation of the ARN/ $\text{Ca}^{2+}$  interfacial gel (less than ca. 0.03 wt. % to reach  $E'$  below 40 mN/m), more for D and even more for E.

The data allow to conclude that there is no correlation between the interfacial activity of crude oils and their interfacial gel inhibition activity. Indeed, as mentioned above from the results presented in figures 2, the IFT of crude oils D, E, and U in solution in xylene are relatively similar while B is significantly more surface active. Consequently, there is no link between this order and the inhibition efficiency (figure 4).

It was previously shown that asphaltenes and naphthenic acids could inhibit the formation of ARN/ $\text{Ca}^{2+}$  interfacial gel<sup>30, 31</sup>. The crude oil E has the lowest TAN value (indicative of the concentration of naphthenic acid in crude oil) and the second lowest asphaltene content and has the lowest inhibition efficiency among the 4 crude oils considered in this article which is consistent. However, there is no correlation between the TAN and the asphaltene content on one side and the inhibition efficiency on the other side for the three other crude oils (B, D, and U). However, this point will be better highlighted by selectively removing asphaltenes and/or naphthenic acids from crude oil and subsequently studying the properties of the prepared samples (section 3.1.3).

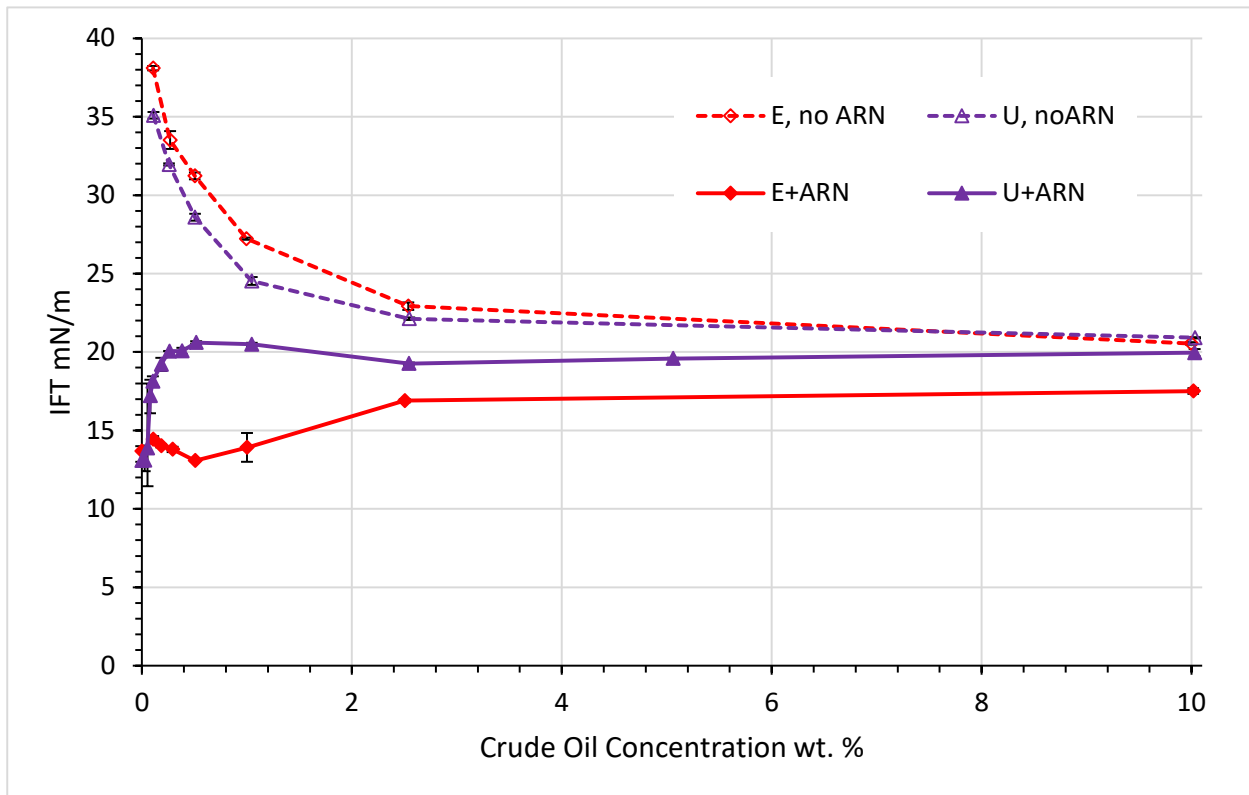
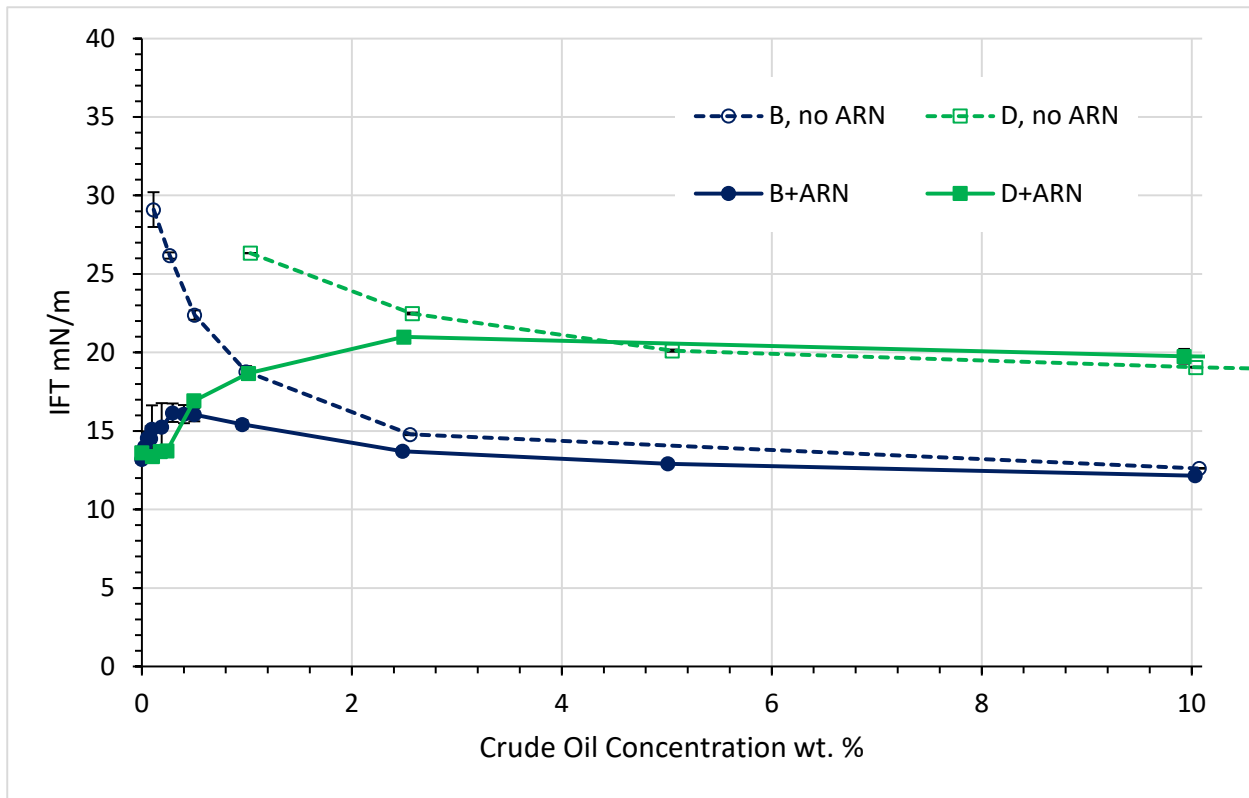


Figure 2: Variations of the IFT measured after 3600 s of adsorption with crude oil concentrations in absence (empty symbols, dotted lines) or in presence (filled symbols, solid lines) of 10  $\mu$ M of ARN. Lines are guides for eyes.

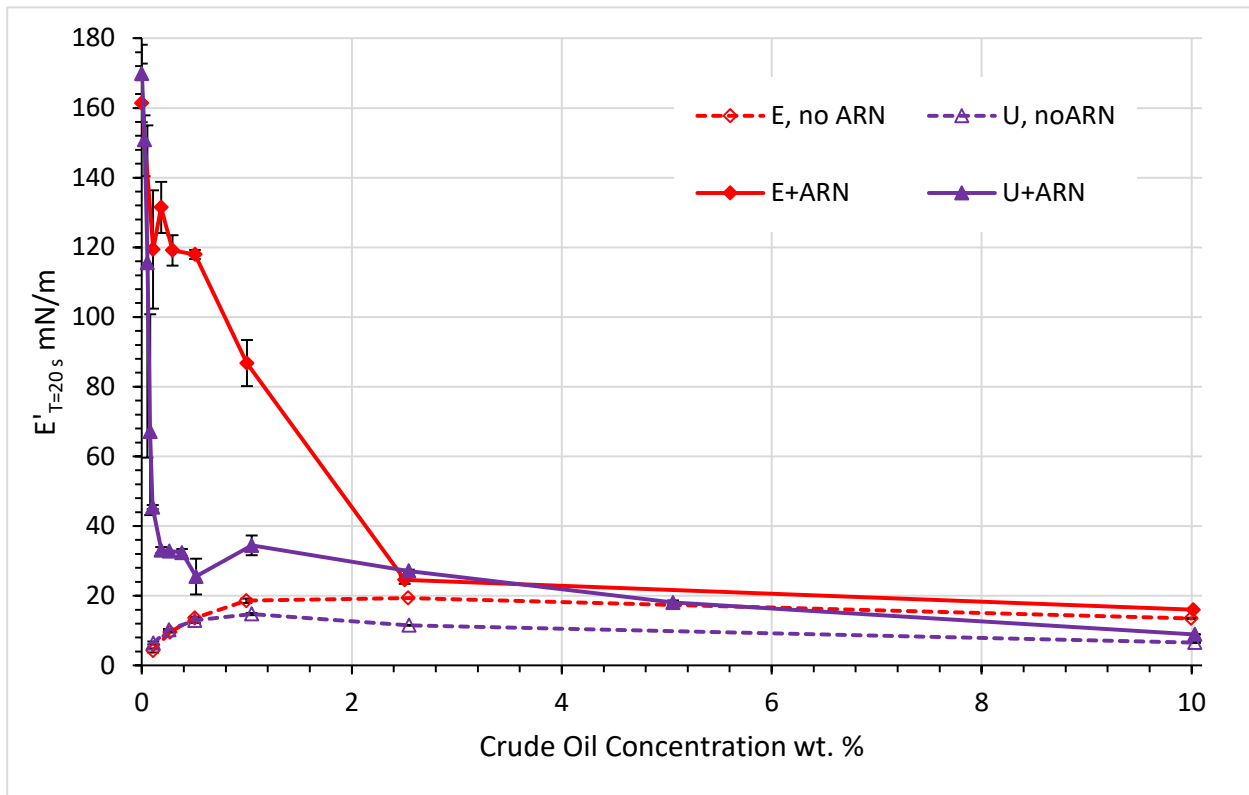
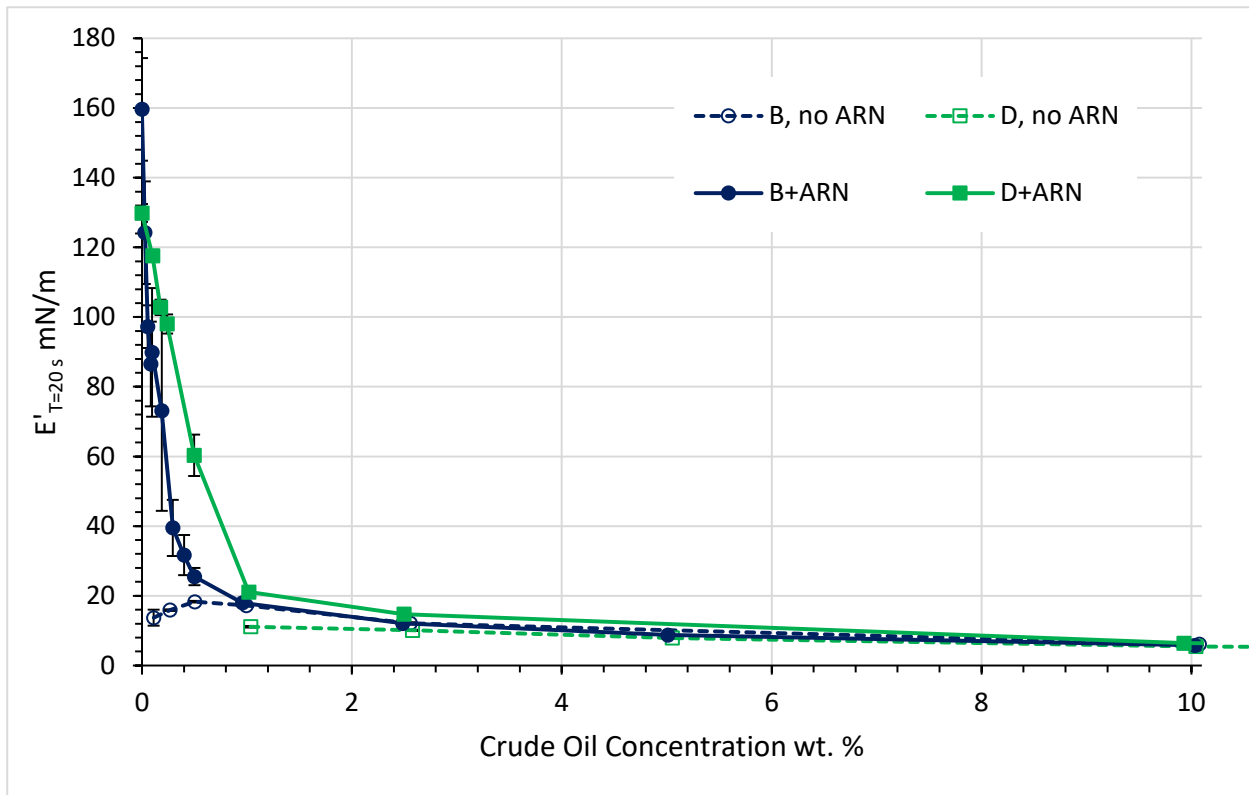


Figure 3: Variations of  $E'$  measured at a period of 20 seconds with crude oil concentrations in absence (empty symbols, dotted lines) or in presence (filled symbols, solid lines) of  $10 \mu\text{M}$  of ARN. Lines are guides for eyes.

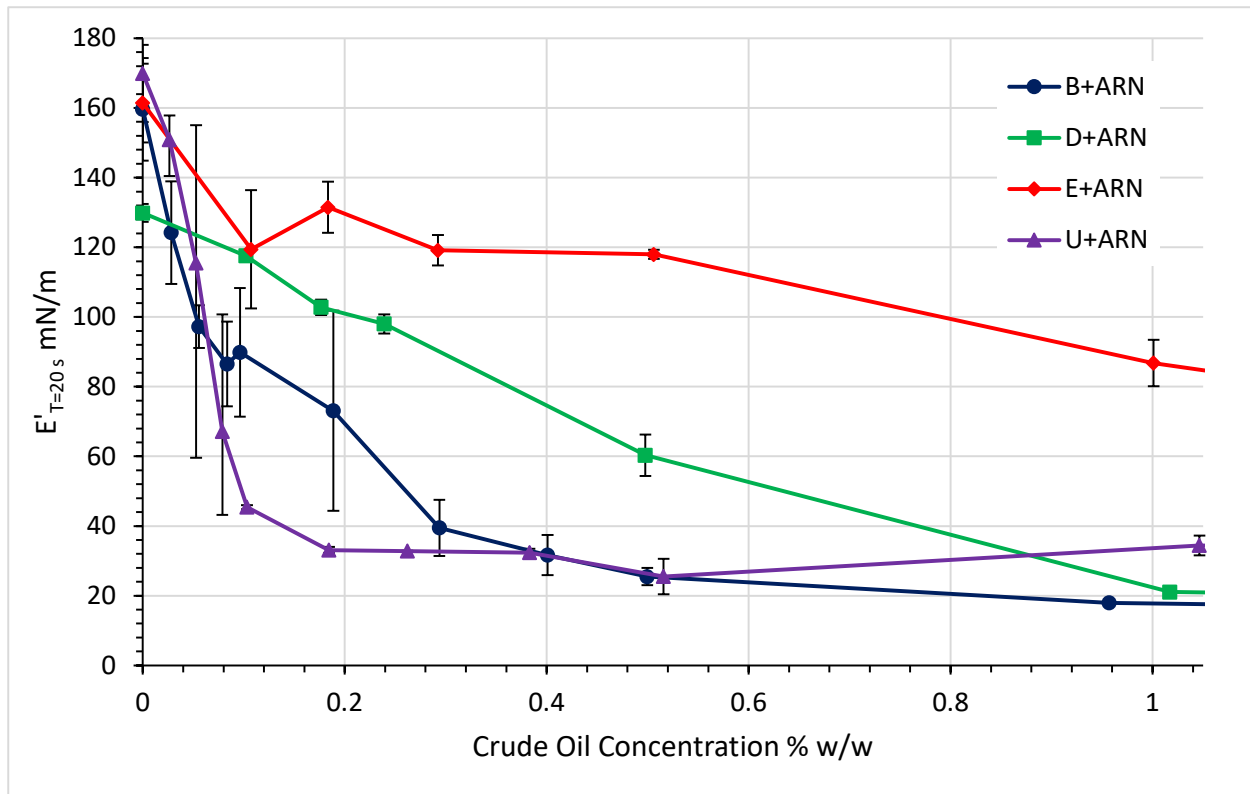


Figure 4: Comparisons of variations of  $E'$  measured at a period of 20 seconds with crude oil concentrations in presence of  $10 \mu\text{M}$  of ARN. Zoom of data already presented in figure 3. Lines are guides for eyes.

### 3.1.3 Influence of Crude Oil Composition. Selective Crude Oil Component Removal

In order to better elucidate the effect of crude oil composition on the ARN/ $\text{Ca}^{2+}$  interfacial gel inhibition efficiency, selective removal of asphaltenes and/or NA on crude oil D and U were performed. 4 samples were prepared: A deasphalted crude oil was prepared from crude oil D (codename: D-Asp). Naphthenic acids were removed from crude oils D and U (D-NA and U-NA). Finally, both asphaltenes and naphthenic acids were removed from crude oil D (D-Asp-NA); asphaltenes being removed first. Table 2 presents the characteristics of the prepared samples. The yield compares the mass recovered after drying and the initial mass of crude oil. TAN is measured after drying for the samples whose the NA have been removed. Finally, the asphaltene contents recovered on the filters were determined for all the deasphalted samples.

Samples	Density at 25°C (g/cm <sup>3</sup> ) <sup>b</sup>	Yield (wt. %)	TAN (mg <sub>KOH</sub> /g <sub>crudeoil</sub> )	Asphaltenes iC <sub>6</sub> (wt. %)
D-Asp	0.9209	93.1	n.d. <sup>c</sup>	1.42 ± 0.06
D-NA	0.9463	99.9	b.d.l. (<0.1) <sup>d</sup>	n.d.
D-Asp-NA	0.9465	98.9 (99.1 after deasphalting) <sup>e</sup>	b.d.l. (<0.1)	1.47 ± 0.02 (measured after deasphalting)
U-NA	0.9552	97.1	b.d.l. (<0.1)	n.d.

**Table 2:** Characteristics of the samples prepared by removing asphaltenes and/or naphthenic acids. The asphaltene content values are the average of 4 to 7 measurements and the error bars are the standard deviations of the measurements.

As indicated in Table 2, the content of asphaltene removed in D-Asp and D-Asp-NA is similar to the independently determined content of asphaltenes in this crude oil (table 1) which means that the asphaltenes were successfully removed in these samples. The TAN in samples D-NA, D-Asp-NA, and U-NA are low (lower than the detection limit of the determination method), here also indicating that (most of) NA have been removed in these samples. Finally, it is worth mentioning that the density of U-NA is significantly higher than the value determined for the actual crude oil (0.9552 vs. 0.8772 g/cm<sup>3</sup> at 25°C) which is attributed to the presence of residual solvent (dichloromethane) and/or evaporation of the most volatile components of crude oil U.

Figure 5 presents the variations of IFT with crude oil concentration with and without 10 μM ARN for crude oil D and its derivatives (D-Asp, D-NA, D-Asp-NA) while E' moduli for the same systems, but only in presence of ARN, are shown in figure 6. The E' moduli in absence of ARN are not indicated since they are low (less than 12 mN/m) and do not provide extra-information. It can be seen that the IFT for samples D and D-Asp are significantly lower than for samples containing no NA i.e. D-NA and D-Asp-NA. It can therefore be concluded that NA controls the interfacial properties of crude oil at the tested conditions i.e. at pH=8. This statement must depend on conditions, primarily on pH. Indeed, in basic medium, NA are ionized (carboxylate), the ionization rate depending on the pH value, and their surface activity is significantly higher than when they are under acid form<sup>43, 44</sup>.

The shape of the variations of IFT and E' with concentration for samples whose asphaltenes and/or NA have been removed are qualitatively similar to the "unmodified" crude oils. IFT of systems containing 10 μM of ARN are constant at around 13-14 mN/m then increases when modified crude oils are present reaching values similar to systems which do not contain ARN. The only exception concerns D-Asp-NA whose the IFT values with and without ARN are still significantly different at 10 wt. %. E' moduli

<sup>b</sup> Due to low sample amount, the densities were only measured one time.

<sup>c</sup> n.d.: non determined.

<sup>d</sup> b.d.l.: below detection limit.

<sup>e</sup> Concerning D-Asp-NA, the yield of the deasphalting was 99.1 %. Then NA was removed from this sample and the yield of this step was 99.8 %. The total yield of both steps was therefore 98.9 %.

are constant at low crude oil concentrations (ca. 130 mN/m) and then decreases at higher concentrations. Consequently, the behaviors identified in section 3.1.2 are valid for asphaltenes and/or NA-removed samples.

This similarity in behavior allows to determine the contribution of the respective fractions on the ARN/Ca<sup>2+</sup> inhibition efficiency. The inhibition efficiency order of the samples considered in figures 5 and 6, assessed from the onset of IFT increases and E' decrease, is D (highest inhibition) > D-Asp > D-NA > D-Asp-NA (lowest inhibition). It can therefore be concluded that NA has a more important contribution in the inhibition than asphaltenes, at least for crude oil D. It is also worth noticing that even if D-Asp-NA has a very reduced potential to inhibit the formation of interfacial gel, i.e. high sample concentration is necessary to significantly reduce E', it is non-null. That means crude oil D have other components than asphaltenes and NA that are able to inhibit the interfacial gel formation, albeit at a lower level. This conclusion is valid for the experimental definition of asphaltenes used in this article (insoluble in n-hexane). Owing to the asphaltene polydispersity<sup>45</sup>, other procedures to remove asphaltenes could have perhaps led to different results.

Naphthenic acids were also removed from the crude oil U to prepare U-NA. U was selected because it has the highest inhibition efficiency among the 4 crude oils (figure 4) and has a very low asphaltene content (0.08 wt. %). The IFT and E' variations with crude oil concentration are shown in figures 7 and 8 respectively. These two figures allow to draw conclusions similar to those obtained with D-NA sample. Indeed, NA also controls the surface activity of crude oil U at pH=8 as shown by the highest surface activity for U compared with U-NA. In addition, NA has an active role in the inhibition of ARN/Ca<sup>2+</sup> interfacial gel (figure 8, onset of E' decrease is shifted to higher concentrations in the case of U-NA) but other components present in U also participate to the inhibition since E' would finally be strongly reduced if enough U-NA is present.

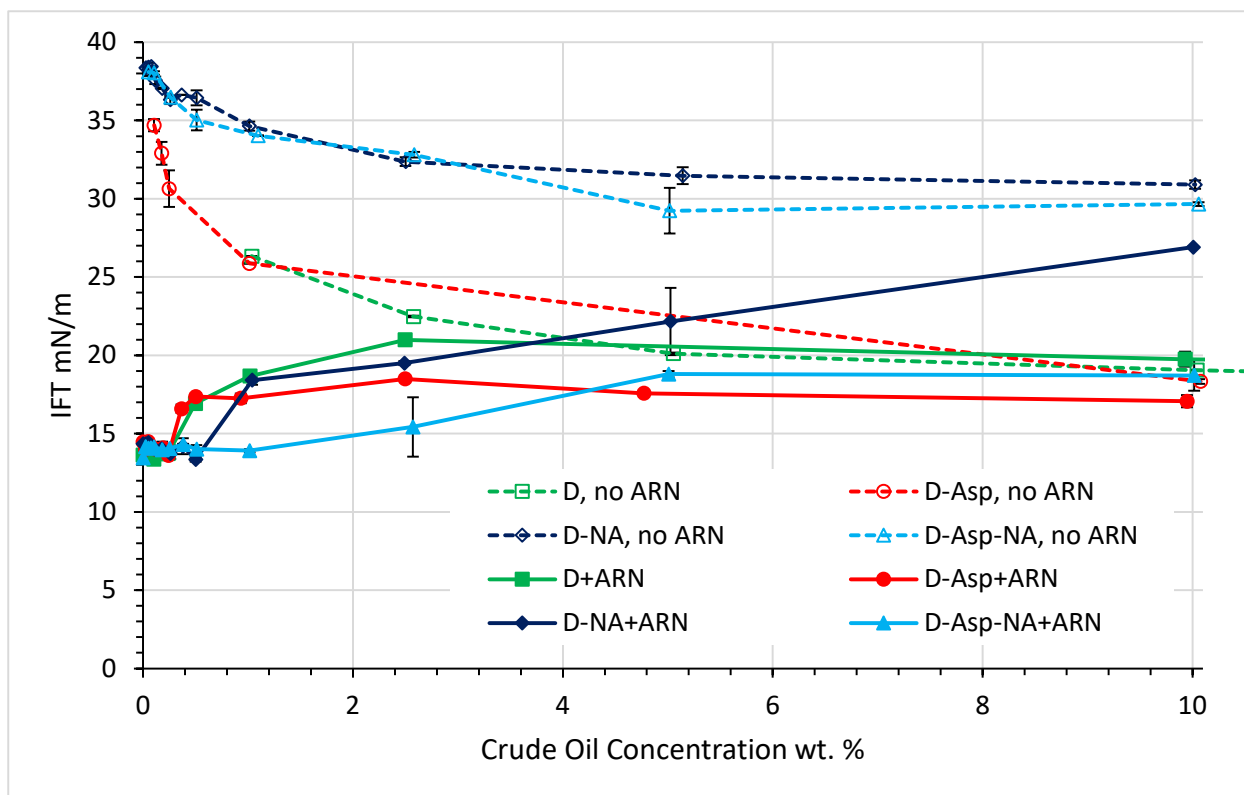
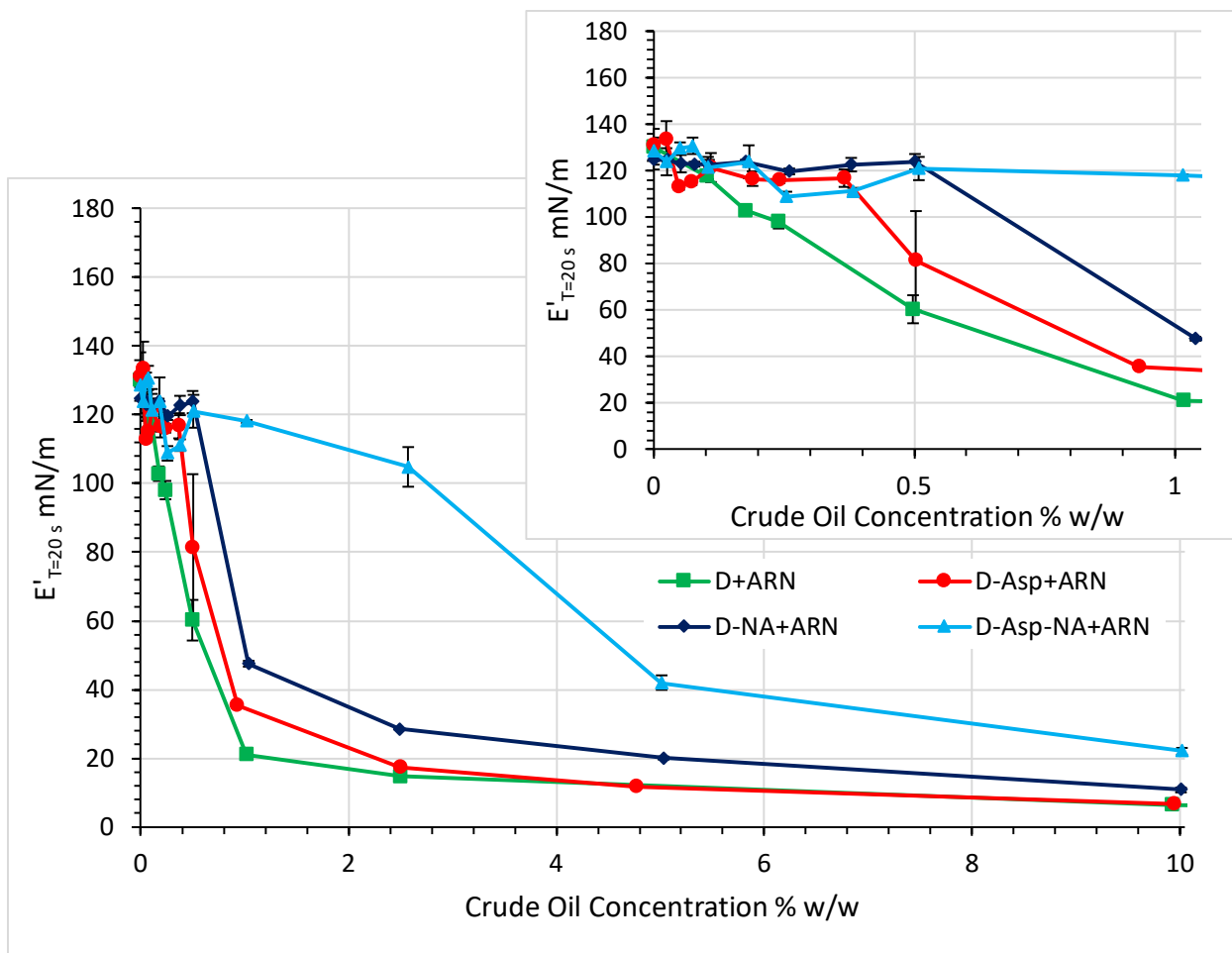


Figure 5: Variations of the IFT measured after 3600 s of adsorption with crude oil concentrations in absence (empty symbols, dotted lines) or in presence (filled symbols, solid lines) of 10 μM of ARN for crude oil D and its derivatives (D-Asp, D-NA, and D-Asp-NA). Lines are guides for eyes.





**Figure 6:** Comparisons of variations of  $E'$  measured at a period of 20 seconds with crude oil concentrations in presence of  $10 \mu\text{M}$  of ARN for crude oil D and its derivatives (D-Asp, D-NA, and D-Asp-NA). Insert: Zoom at low crude oil concentrations. Lines are guides for eyes.

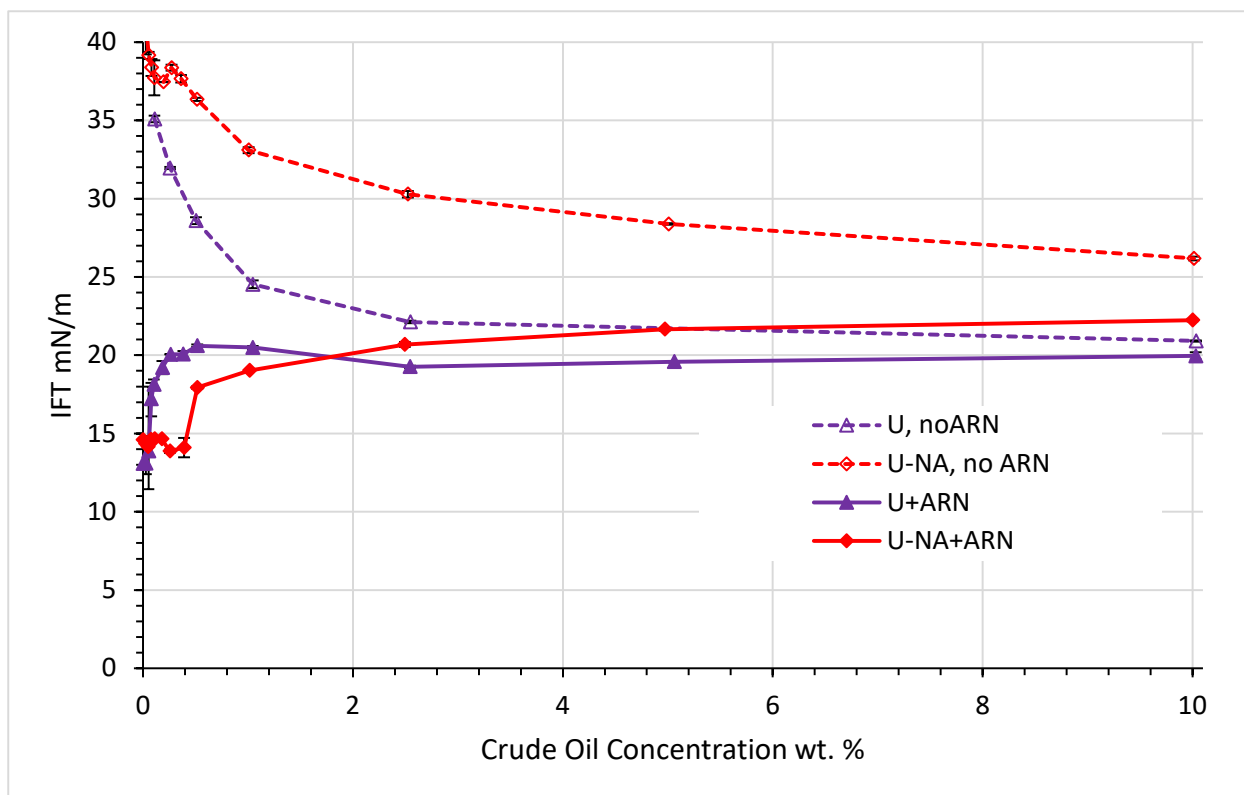


Figure 7: Variations of the IFT measured after 3600 s of adsorption with crude oil concentrations in absence (empty symbols, dotted lines) or in presence (filled symbols, solid lines) of 10  $\mu$ M of ARN for crude oil U and its derivative U-NA. Lines are guides for eyes.

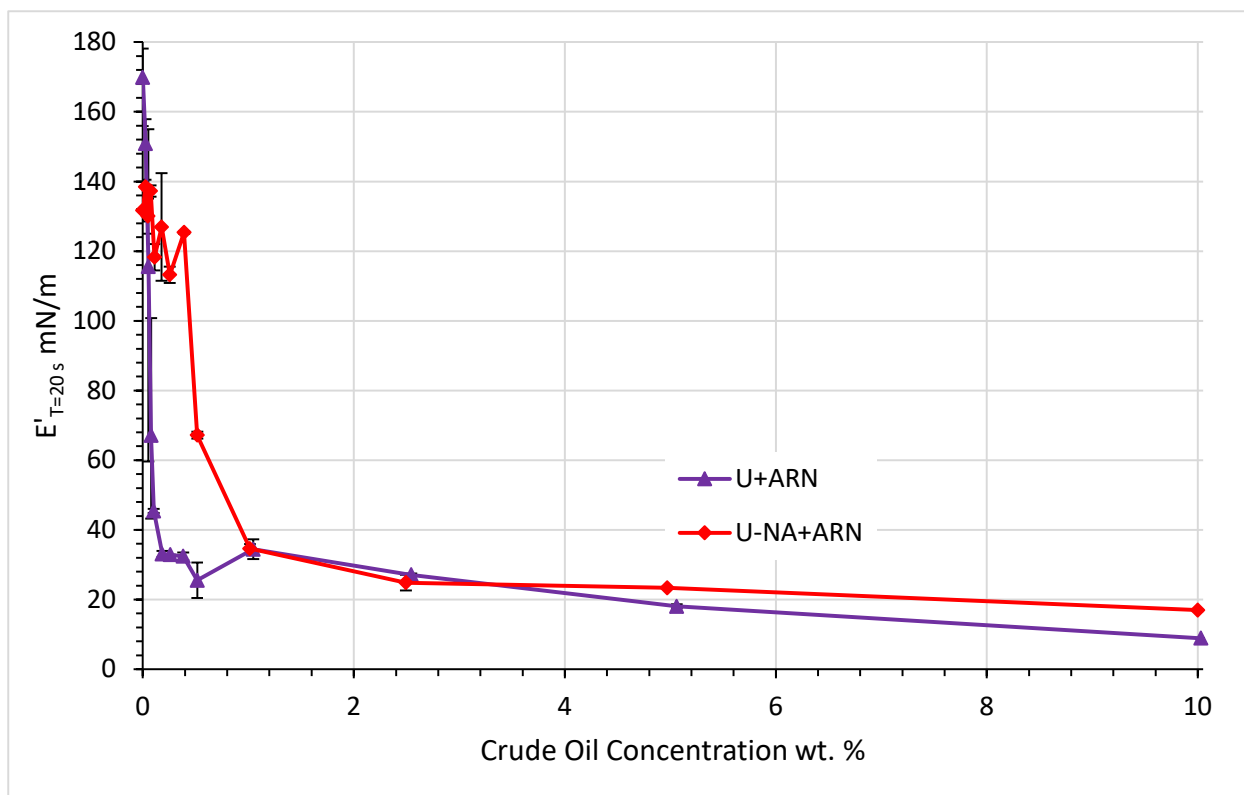


Figure 8: Comparisons of variations of  $E'$  measured at a period of 20 seconds with crude oil concentrations in presence of  $10 \mu\text{M}$  of ARN for crude oil U and its derivative U-NA.

### 3.1.4 Definition of an Inhibition Parameter

After presenting the qualitative effect of asphaltene and NA fractions on the interfacial gel inhibition, this section aims to quantify their respective effects. First, a parameter representing the interfacial gel inhibition efficiency is introduced. This is defined as the crude oil concentration required to significantly reduce the gel strength characterized by  $E'$ . Based on the figures 6 and 8, it was conveniently chosen a value of  $40 \text{ mN/m}$  since below this value, the variations of  $E'$  with concentrations steeply level off. As the exact concentrations where  $E'=40 \text{ mN/m}$  were not directly measured, assessments of the  $C_{\text{inh}}$  values were calculated from data presented in figures 4, 6, and 8 by performing a linear regression between the two points framing  $40 \text{ mN/m}$  (table 3). The asphaltenes and NA concentrations at  $C_{\text{inh}}$  are also shown in table 3.

Crude oil	C <sub>inh</sub> wt. %	C <sub>Asp</sub> at C <sub>inh</sub> μM	C <sub>NA</sub> at C <sub>inh</sub> μM
B	0.29	184	128
D	0.77	138	231
E	2.1	81	105
U	0.14	1.3	30
D-Asp	0.89	-	-
D-NA	1.6	-	-
D-Asp-NA	5.5	-	-
U-NA	0.93	-	-

**Table 3:** Values of the inhibition parameter, i.e. concentration of crude oil at which  $E'_{T=20s}=40$  mN/m. The concentrations of asphaltenes  $C_{Asp}$  and naphthenic acids  $C_{NA}$  at this concentration are also indicated. A molecular weight of 750 g/mol was assumed<sup>46, 47</sup> to calculate  $C_{Asp}$ .

Table 2 indicates that the concentrations of asphaltenes and naphthenic acids for crude oils B, D, and E at inhibition point are all relatively similar, in the order of 100 μM, which could indicate that asphaltenes and naphthenic acids have similar effects in these crude oils. On the contrary, the concentrations of these two classes of components at inhibition point for crude oil U are significantly lower especially for asphaltenes. This could perhaps indicate that some specific components present in crude oil U have a significant impact on the inhibition of ARN/Ca<sup>2+</sup> interfacial gel.

A simplistic model was then developed to quantitatively calculate the contribution of every class of components on the inhibition efficiency using data on asphaltenes and/or NA-removed samples presented on table 3. As mentioned above, the ARN/Ca<sup>2+</sup> gel is inhibited due to the presence of crude oil components that adsorb at the interface in sufficiency high concentration to prevent the connection and cross-linking between ARN molecules at the interface. Naphthenic acids probably act as termination agent of the cross-linked network formed between ARN and Ca<sup>2+</sup><sup>23</sup>. Asphaltenes could act similarly, indeed a fraction of asphaltene molecules bears COOH function, or by just adsorbing which would increase the average distance between ARN molecules at the interface. In addition, asphaltenes can interact with ARN in the bulk preventing the latter to access the interface<sup>20</sup>.

The adsorbed amount at interface ( $\Gamma_T$ ) is the sum of ARN reacting with Ca<sup>2+</sup> ( $\Gamma_{ARN}$ ) and all the crude oil components that have the ability to inhibit the gel formation gathered together in the same term ( $\Gamma_{CO}$ ):

$$\Gamma_T = \Gamma_{ARN} + \Gamma_{CO} \quad (1)$$

Assuming for simplicity sake that the adsorption can be described by Langmuir isotherms, then<sup>39</sup>:

$$\Gamma_T = \Gamma_m \frac{K_{L,ARN} \cdot C_{ARN}}{1 + K_{L,ARN} \cdot C_{ARN} + K_{L,CO} \cdot C_{CO}} + \Gamma_m \frac{K_{L,CO} \cdot C_{CO}}{1 + K_{L,ARN} \cdot C_{ARN} + K_{L,CO} \cdot C_{CO}} \quad (2)$$

With  $\Gamma_m$ : maximum adsorbed amount at the interface,  $K_{L,ARN}$  and  $K_{L,CO}$ : the equilibrium adsorption constants for ARN and the crude oil components, and  $C_{ARN}$  and  $C_{CO}$ : the bulk concentration of ARN and

crude oil components that can inhibit the gel formation. It must be mentioned that the adsorption of ARN when gel is formed cannot most likely be modelled by the Langmuir equation since there is cross-linking, but around the inhibition point, the connection between ARN molecules would be limited and the validity of this equation to model ARN adsorption would be more plausible. It must be noticed that the Langmuir isotherm has been found to correctly fit IFT data for several crude oil components such as asphaltenes<sup>48, 49</sup> and for model naphthenic acid (stearic acids)<sup>35</sup>.

In order to inhibit the gel formation, the adsorption of crude oil components and therefore the right terms in equations (1) and (2) must be high enough. As, in the interfacial tests presented in this article, the ARN concentration is constant (10  $\mu\text{M}$ ), it is the term  $K_{L,CO} \cdot C_{CO}$  that dictates if the gel is inhibited. Consequently, this term and therefore  $C_{CO}$  must reach a minimum value to inhibit the gel formation. This minimum concentration will be called  $C_{\text{Critical}}$ .

It is then assumed that the contributions of the respective crude oil components on the inhibition are additive (no interaction/synergy):

$$C_{\text{eff\_Asp}} + C_{\text{eff\_NA}} + C_{\text{eff\_matrix}} = C_{CO} \quad (3)$$

With  $C_{\text{eff\_Asp}}$ ,  $C_{\text{eff\_NA}}$ , and  $C_{\text{eff\_matrix}}$ : effective concentrations of asphaltenes, NA, and the matrix, i.e. all the other components, on the inhibition. The “effective” term encompasses the bulk concentration of the considered compound but also its adsorption constant ( $K_L$  in equation (2)), and its ability to inhibit the gel formation once adsorbed.

By introducing the effective mass fractions of the components present in the crude oil:

$$\left( \phi_{NA} + \phi_{Asp} + \phi_{\text{matrix}} \right) \cdot C_{\text{Crude Oil}} = C_{\text{eff\_Asp}} + C_{\text{eff\_NA}} + C_{\text{eff\_matrix}} \quad (4)$$

At inhibition, we have:

$$C_{\text{Crude Oil}} = C_{\text{Inh}} \quad (5)$$

Hence:

$$\frac{\left( \phi_{NA} + \phi_{Asp} + \phi_{\text{matrix}} \right)}{C_{\text{Critical}}} = \frac{1}{C_{\text{Inh}}} \quad (6)$$

By introducing  $C_{\text{Inh}_D}$ ,  $C_{\text{Inh}_D\text{-Asp}}$ ,  $C_{\text{Inh}_D\text{-NA}}$ , and  $C_{\text{Inh}_D\text{-Asp-NA}}$  the inhibition concentration for systems D, D-Asp, D-NA, and D-Asp-NA and considering the fact that the term  $\phi_{NA}$  is not present for D-NA and D-Asp-NA and  $\phi_{Asp}$  is not present for D-Asp and D-Asp-NA, the respective contributions of the fractions can be calculated:

$$\frac{\left( \phi_{NA} + \phi_{\text{matrix}} \right)}{\left( \phi_{NA} + \phi_{Asp} + \phi_{\text{matrix}} \right)} = \frac{C_{\text{Inh}_D}}{C_{\text{Inh}_D\text{-Asp}}} \quad (7)$$

$$\frac{\left( \phi_{Asp} + \phi_{\text{matrix}} \right)}{\left( \phi_{NA} + \phi_{Asp} + \phi_{\text{matrix}} \right)} = \frac{C_{\text{Inh}_D}}{C_{\text{Inh}_D\text{-NA}}} \quad (8)$$

$$\frac{(\phi_{matrix})}{(\phi_{NA} + \phi_{Asp} + \phi_{matrix})} = \frac{C_{Inh\_D}}{C_{Inh\_D-Asp-NA}} \quad (9)$$

The results are presented in table 4. Values show that NA have the most important contribution to the inhibition, around twice as much as the asphaltenes. The other components have a relative minor influence on inhibition of crude oil D (14 %). It must be noticed that the sum of individual contributions is higher than 100 % which could be attributed to the uncertainties associated to the determination of  $C_{Inh}$ , especially its extrapolation, or to the limitation of the model.

The same model (equation (8)) was applied to crude oil U. As shown in table 4, NA represents 85 % of the inhibition potential in this oil. Asphaltene contribution should be minor which is consistent with the very low concentration of this class of compounds in U (table 1).

Crude oil	Components	Contribution to inhibition
D	NA + Matrix	86 %
	Asp + Matrix	48 %
	Matrix	14 %
U	Asp + Matrix	15 %

**Table 4:** Contribution of the asphaltenes, naphthenic acids, and the “matrix” i.e. other components in the inhibition of ARN/ $Ca^{2+}$  interfacial gel.

### 3.2 Bottle Testing

The interfacial tension and interfacial dilational rheology experiments have allowed to put into evidence differences of inhibition efficiency between the different studied crude oils. However, it is important to study how these differences correlate with calcium naphthenate deposition issues in crude oil production and processing. It was therefore attempted to upscale the results presented in section 3.1 by performing bottle test. However, experimental conditions for bottle tests had to be adjusted and consequently there are significant differences between the two techniques. The most significant is the fact the ARN concentration was increased 10 folds to 100  $\mu$ M in bottle tests, a decision based on previous bottle test experiments<sup>27</sup> to make the detection of deposit easier. Another difference is the absence of shaking in experiments performed with the SINTERFACE apparatus.

In absence of crude oil (only 100  $\mu$ M ARN in the xylene phase), some turbid material was visible indicating the presence of a precipitate formed by reaction between ARN and  $Ca^{2+}$  (figure S1 in supporting material) which is consistent with literature<sup>27, 29</sup>. The turbid material is not present in absence of ARN. It was found difficult to transfer these mixtures to centrifugation tubes since many “microgels” were stuck

to the glass wall and consequently were not included in later analysis. This problem was not found when crude oil is also present.

When crude oil and ARN are both present, the aqueous phase was found non-turbid after centrifugation. In addition, it was noticed, for most of the samples, the presence of a brownish material on the wall of the centrifugation tubes. In the case of crude oil U + ARN systems, this brownish material can be pushed with a spatula or a pipette and recovered. Part of this material was transferred to microscope slide (figure 9.a). This material seems to be a soft solid and seems to be formed by reaction between ARN and  $\text{Ca}^{2+}$  since it is not present in absence of ARN (see below). This specific material was observed by microscopy (figure 9.b). The microscopic pictures indicate that this object is 3-dimensional but it seems to be “multi-layered”. It confirms the compact nature of the material with the presence of only one phase and also that no droplet for instance is trapped. This fact and the absence of droplet in the system U+ARN after centrifugation, which is different from the equivalent systems in absence of ARN (see below), confirms that the ARN/ $\text{Ca}^{2+}$  gel has destabilizing effect on crude oil emulsion. The soft solid material is present for all the crude oil U volume fraction tested and have the same aspect under microscope (from 0.05 to 0.5, see figures S2 and S3).

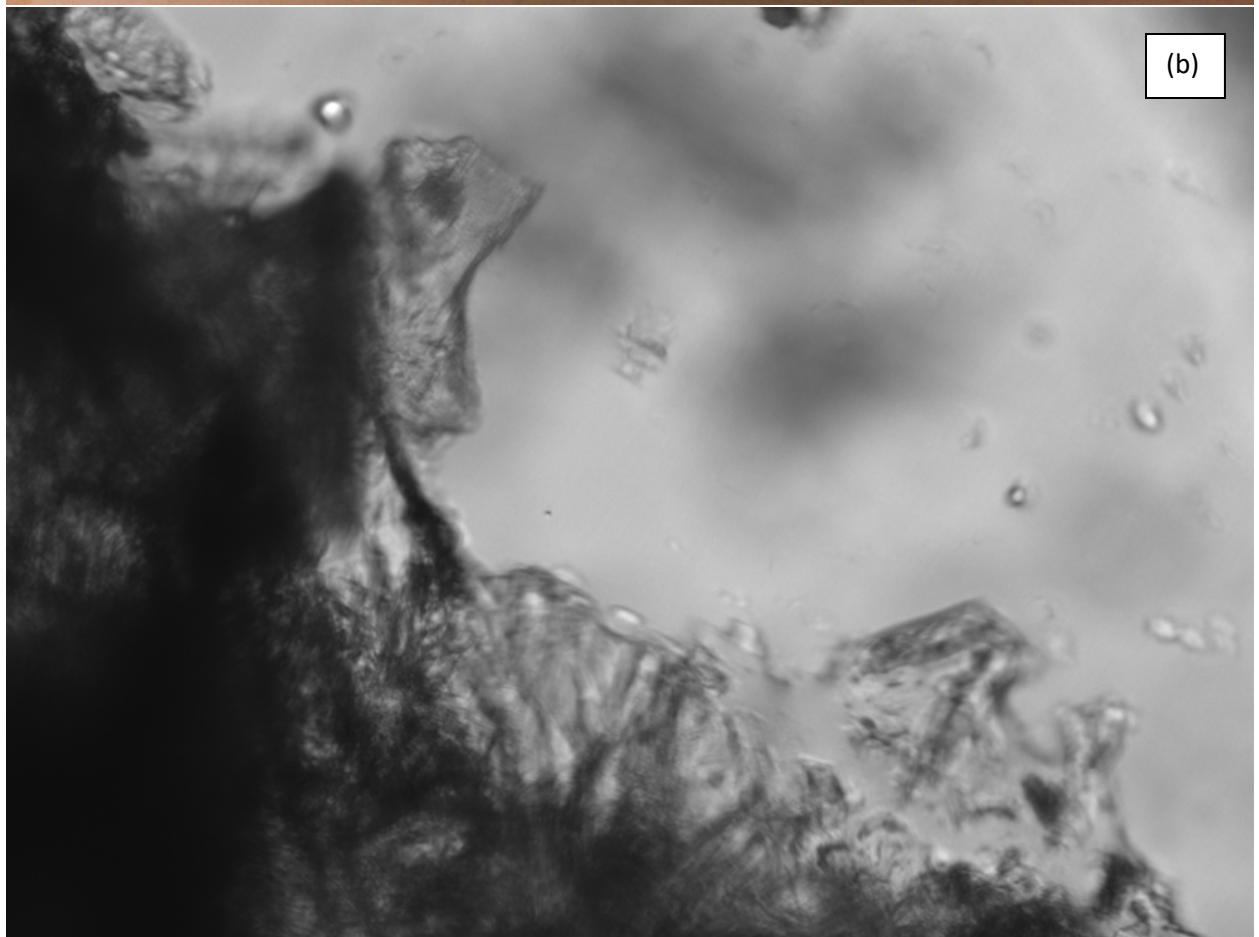
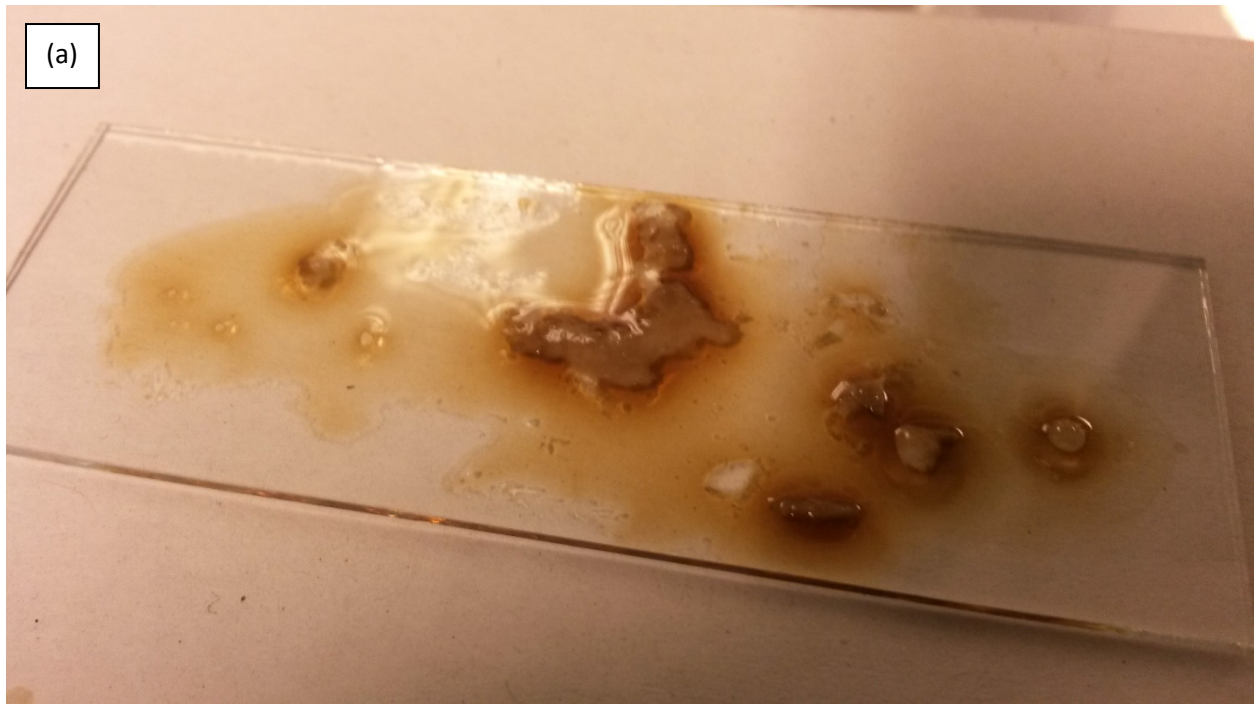




Figure 9: Material recovered from the wall of the centrifugation tube for crude oil U (volume fraction=0.1) in presence of 100  $\mu\text{M}$  of ARN and transferred on a microscope slide (a). The brownish material was then observed under microscopy. Note absence of droplets compared with systems in absence of ARN presented in figure S9 (b). Dimension of the picture: 647 $\times$ 479  $\mu\text{m}$ .

The same soft materials were observed for the crude oils D and E in presence of ARN (the crude oil B was not tested) at low crude oil volume fractions. For crude oil D, at a volume fraction higher than 0.2, the material present in the centrifugation tube wall “disintegrates” when it is pushed with a spatula or a pipette. Consequently, it was difficult to recover the material on microscope slides. However, the same material was easily visible by microscopy (figures S4 and S5). Finally, concerning crude oil E in presence of ARN, the material that is present on centrifugation tube wall at volume fractions of 0.4 and 0.5 seems to be more fluffy than for lower crude oil component and the material that can be recovered from the microscope slides form smaller objects (small brownish particles) than at lower volume fraction (figures S6 and S7).

When recovering the material, it was felt that their amount was disproportionate compared with the low amount of ARN present in every tube (1.2 mg). Consequently, it was decided to recover as much material as possible from the centrifugation tube wall and determine the content of volatile compounds in the soft solid material by evaporating them at 60°C for 1 day. The recovered masses are a strong underestimation of the real masses of the material visible on the tube wall, but it is a simple test to determine if other compounds than ARN is present. The results are summarized in table 5. The recovered objects are systematically heavier than the total ARN mass present in every sample, 60-70 times heavier for U, even if all the objects have not been recovered. That means that the network formed by ARN and  $\text{Ca}^{2+}$  has incorporated other component(s) in these soft solid materials. These other components are volatile since they represent around 98 wt. % of the materials. Consequently, the soft solid materials formed by ARN and  $\text{Ca}^{2+}$  in presence of crude oil are ARN- $\text{Ca}^{2+}$  gel swollen by solvent.

Crude oil	Mass material recovered mg	Mass dried recovered material mg	% non-volatile
D, run 1	8.0	0.2	2.(5)
D, run 2	10.7	0.3	2.(8)
E, run 1	37.4	0.5	1.(3)
E, run 2	30.2	0.5	1.(7)
U, run 1	83.2	1.6	1.(9)
U, run 2	87.8	1.8	2.(1)

Table 5: Masses of material recovered from the centrifugation tube walls for crude oil at a volume fraction of 0.1 + 100  $\mu$ M ARN systems and then put in an oven for 1 day at 60°C. Due to the low dried mass, the calculated % non-volatile only provides an order of magnitude.

Finally, bottle tests were performed in absence of ARN to be used as references. Brownish material is also visible on the walls of the centrifugation tubes, but they do not seem to be as solid as proved by the fact as they are not visible when transferred on a microscope slide (figures S8). Microscope observations (figure S9) indicate the presence of droplets in these samples, which were absent in the presence of ARN. No solid material as those present in ARN systems (figure 9.b) are visible albeit some “wrinkles “-like structures are visible around droplets for crude oils E and U. These “wrinkles cannot be confounded with the solids formed by ARN and are perhaps viscoelastic materials present at the oil/water interface that can be formed by, for instance, asphaltenes<sup>50</sup>.

## 4 Discussion and Conclusion

One of the initial steps in calcium naphthenate deposition is the reaction between ARN and  $\text{Ca}^{2+}$  resulting in the formation of an interfacial gel. This gel will then grow to ultimately result in the formation of solid deposit. It was previously shown that crude oil components, namely asphaltenes and naphthenic acids, can inhibit the formation of the interfacial gel. This inhibition by crude oil components could explain why calcium naphthenate deposition is not observed in some oil fields despite the presence of ARN in these systems<sup>22</sup>. Consequently, the interfacial gel inhibition by 4 real crude oils spanning a large range of properties (TAN, density, asphaltene content) was studied.

The inhibition ability of crude oils was determined as the crude oil amount necessary to significantly reduced the  $E'$  modulus of interfacial gel formed by the reaction between ARN and  $\text{Ca}^{2+}$ . It was found that the 4 tested crude oils display different inhibition abilities and they could be ranked as a function of their inhibition ability:  $U \approx B > D > E$ . This order is not directly related to the total asphaltene and naphthenic acid contents of the crude oils and therefore cannot be directly predicted by performing

simple chemical analysis of the oils. The selective extraction of asphaltenes and/or naphthenic acids from crude oils have allowed to determine that naphthenic acids are the most prevalent inhibitors in the tested crude oils followed by asphaltenes. Other crude oil components which are still unidentified are also involved in the inhibition by crude oils but their effects are relatively minor but non-null.

All these observations make us think that the procedure presented in the article and involving interfacial tension and interfacial rheology measurements (figure 4 and table 3) could be used as a simple screening method to compare the inhibition potentials of crude oil. This could be used, for instance, in a larger flow assurance strategy aiming to determine the risk of calcium naphthenate deposition in new fields to be developed<sup>12</sup>.

An important point in the prediction of calcium naphthenate deposition is to determine how the results obtained at the interface scale control the full-scale process. This is why some bottle tests were performed. In these tests, the ARN concentration was increased tenfold compared with interfacial experiments to be able to visually detect the presence of precipitate. It was found that some soft solid material was formed even in presence of crude oil U at a volume fraction of 0.5 (figures S2 and S3). This soft solid material formed by ARN and  $\text{Ca}^{2+}$  in presence of crude oil are ARN- $\text{Ca}^{2+}$  gel swollen by solvent. The same material is formed in presence of crude oil D and E, but their formation seems to be inhibited if enough of these crude oils are present (figures S4 to S7). It would be important to quantify the amount of ARN and  $\text{Ca}^{2+}$  in these materials to better understand their properties.

Interfacial measurement indicates that a crude oil U concentration of 0.14 wt. %, equivalent to a volume fraction of  $1.4 \cdot 10^{-3}$ , is able to inhibit the formation of ARN/ $\text{Ca}^{2+}$  interfacial gel (table 3). Bottle tests, on the contrary, indicate the presence of solid material formed by reaction between ARN and  $\text{Ca}^{2+}$  for crude oil U volume fraction of 0.5. Even if the ARN concentration is tenfold higher in bottle test experiments, these results are not consistent with each other. One method would indicate that crude oil U strongly inhibit the formation of ARN/ $\text{Ca}^{2+}$  interfacial gel, while the second would indicate that U would not have the same impact on the formation of solid deposit. This means a better understanding of the ARN/ $\text{Ca}^{2+}$  system is required to be able to extrapolate the results obtained at the interface to bigger scales. In addition, the bottle tests performed in this work only provide qualitative measurements. More developments are required to make the method quantitative

## 5 Acknowledgments

The authors thank Total S.A. and Total E&P Norge AS for financial support of the present work and the permission to publish the work.

## 6 Supporting Information

- Pictures of mixtures of xylene solutions containing no (right) or 100  $\mu\text{M}$  ARN and aqueous phases after shaking overnight.

-Photographic and microscope pictures of material recovered from the wall of centrifugation tubes after shaking overnight aqueous and xylene solutions. The xylene solutions contained crude oil at various concentrations and 100 µM of ARN.

## 7 References

1. Sjöblom, J.; Simon, S.; Xu, Z. The chemistry of tetrameric acids in petroleum. *Adv. Colloid Interface Sci.* **2014**, *205* (0), 319-338.
2. Eke, W. I.; Victor-Oji, C.; Akaranta, O. Oilfield metal naphthenate formation and mitigation measures: a review. *Journal of Petroleum Exploration and Production Technology* **2020**, *10* (2), 805-819.
3. Lutnaes, B. F.; Brandal, O.; Sjöblom, J.; Krane, J. Archaeal C80 Isoprenoid Tetraacids Responsible for Naphthenate Deposition in Crude Oil Processing. *Org. Biomol. Chem.* **2006**, *4* (4), 616-620.
4. Lutnaes, B. F.; Krane, J.; Smith, B. E.; Rowland, S. J. Structure Elucidation of C80, C81 and C82 Isoprenoid Tetraacids Responsible for Naphthenate Deposition in Crude Oil Production. *Org. Biomol. Chem.* **2007**, *5* (12), 1873-1877.
5. Smith, B. E.; Sutton, P. A.; Lewis, C. A.; Dunsmore, B.; Fowler, G.; Krane, J.; Lutnaes, B. F.; Brandal, Ø.; Sjöblom, J.; Rowland, S. J. Analysis of ARN Naphthenic Acids by High Temperature Gas Chromatography and High Performance Liquid Chromatography. *J. Sep. Sci.* **2007**, *30* (3), 375-380.
6. Baugh, T. D.; Grande, K. V.; Mediaas, H.; Vindstad, J. E.; Wolf, N. O. In *The Discovery of High Molecular Weight Naphthenic Acids (ARN Acid) Responsible for Calcium Naphthenate Deposits*, SPE International Symposium on Oilfield Scale, SPE 93011, Aberdeen, United Kingdom, May 11-12 2005; 2005.
7. Hemmingsen, P. V.; Kim, S.; Pettersen, H. E.; Rodgers, R. P.; Sjöblom, J.; Marshall, A. G. Structural Characterization and Interfacial Behavior of Acidic Compounds Extracted from a North Sea Oil. *Energy Fuels* **2006**, *20* (5), 1980-1987.
8. Qian, K.; Robbins, W. K.; Hughey, C. A.; Cooper, H. J.; Rodgers, R. P.; Marshall, A. G. Resolution and Identification of Elemental Compositions for More than 3000 Crude Acids in Heavy Petroleum by Negative-Ion Microelectrospray High-Field Fourier Transform Ion Cyclotron Resonance Mass Spectrometry. *Energy Fuels* **2001**, *15* (6), 1505-1511.
9. Bertheussen, A.; Simon, S.; Sjöblom, J. Equilibrium Partitioning of Naphthenic Acid Mixture Part 2: Crude Oil-Extracted Naphthenic Acids. *Energy & Fuels* **2018**, *32* (9), 9142-9158.
10. Baugh, T. D.; Wolf, N. O.; Mediaas, H.; Vindstad, J. E.; Grande, K. Characterization of a Calcium Naphthenate Deposit - The ARN Acid Discovery. *Prepr. - Am. Chem. Soc., Div. Pet. Chem.* **2004**, *49* (3), 274-276.
11. Molinier, V.; Loriau, M.; Lescoulié, S.; Martin, B.; Gingras, J. P.; Passade-Boupat, N. Quantification of the Tetraprotic Acids Content in Oils for the Prediction of Naphthenate Deposits Risks. In *International Petroleum Technology Conference*; International Petroleum Technology Conference: Bangkok, Thailand, 2016, p 13.
12. Passade-Boupat, N.; Rondon-Gonzalez, M.; Brocart, B.; Hurtevent, C.; Palermo, T. In *Risk Assessment of Calcium Naphtenates and Separation Mechanisms of Acidic Crude Oil*, SPE International Conference on Oilfield Scale, SPE 155229, Aberdeen, UK, May 30-31 2012.
13. Mapolelo, M. M.; Rodgers, R. P.; Blakney, G. T.; Yen, A. T.; Asomaning, S.; Marshall, A. G. Characterization of naphthenic acids in crude oils and naphthenates by electrospray ionization FT-ICR mass spectrometry. *Int. J. Mass Spectrom.* **2011**, *300* (2-3), 149-157.
14. Mapolelo, M. M.; Stanford, L. A.; Rodgers, R. P.; Yen, A. T.; Debord, J. D.; Asomaning, S.; Marshall, A. G. Chemical Speciation of Calcium and Sodium Naphthenate Deposits by Electrospray Ionization FT-ICR Mass Spectrometry. *Energy Fuels* **2009**, *23* (1), 349-355.

15. Putman, J. C.; Marshall, A. G. Screening Petroleum Crude Oils for ARN Tetraprotic Acids with Molecularly Imprinted Polymers. *Energy & Fuels* **2016**, *30* (7), 5651-5655.
16. Sutton, P. A.; Rowland, S. J. Determination of the Content of C80 Tetraacids in Petroleum. *Energy Fuels* **2014**, *28* (9), 5657-5669.
17. Simon, S.; Nordgård, E.; Bruheim, P.; Sjöblom, J. Determination of C80 Tetra-Acid Content in Calcium Naphthenate Deposits. *J. Chromatogr., A* **2008**, *1200* (2), 136-143.
18. Mohammed, M. A.; Sorbie, K. S. Thermodynamic Modelling of Calcium Naphthenate Formation: Model Predictions and Experimental Results. *Colloids Surf., A* **2010**, *369* (1-3), 1-10.
19. Mohammed, M. A.; Sorbie, K. S.; Shepherd, A. G. Thermodynamic Modeling of Naphthenate Formation and Related pH Change Experiments. *SPE Prod. Oper.* **2009**, *24* (3), 466-472.
20. Wei, D.; Orlandi, E.; Barriet, M.; Simon, S.; Sjöblom, J. Aggregation of tetrameric acid in xylene and its interaction with asphaltenes by isothermal titration calorimetry. *J. Therm. Anal. Calorim.* **2015**, *122* (1), 463-471.
21. Vindstad, J. E.; Grande, K. V.; Høvik, K. M.; Kummernes, H.; Mediaas, H. In *Calcium Naphthenate Management*, 8th International Conference on Petroleum Phase Behavior and Fouling, Pau (France), June 10-14 2007.
22. Brocart, B.; Bourrel, M.; Hurtevent, C.; Volle, J.-L.; Escoffier, B. ARN-Type Naphthenic Acids in Crudes: Analytical Detection and Physical Properties. *J. Dispersion Sci. Technol.* **2007**, *28* (3), 331 - 337.
23. Brocart, B.; Hurtevent, C. Flow Assurance Issues and Control with Naphthenic Oils. *J. Dispersion Sci. Technol.* **2008**, *29* (10), 1496 - 1504.
24. Brandal, O.; Hanneseth, A.-M. D.; Hemmingsen, P. V.; Sjöblom, J.; Kim, S.; Rodgers, R. P.; Marshall, A. G. Isolation and Characterization of Naphthenic Acids from a Metal Naphthenate Deposit: Molecular Properties at Oil-Water and Air-Water Interfaces. *J. Dispersion Sci. Technol.* **2006**, *27* (3), 295 - 305.
25. Nordgård, E. L.; Magnusson, H.; Hanneseth, A.-M. D.; Sjöblom, J. Model Compounds for C80 Isoprenoid Tetraacids: Part II. Interfacial Reactions, Physicochemical Properties and Comparison with Indigenous Tetraacids. *Colloids Surf., A* **2009**, *340* (1-3), 99-108.
26. Simon, S.; Reisen, C.; Bersås, A.; Sjöblom, J. Reaction Between Tetrameric Acids and Ca<sup>2+</sup> in Oil/Water System. *Ind. Eng. Chem. Res.* **2012**, *51* (16), 5669-5676.
27. Simon, S.; Blanco, E.; Gao, B.; Sjöblom, J.; Passade-Boupat, N.; Palermo, T.; Rondon-Gonzalez, M. Rheological Properties of Gels Formed at the Oil/Water Interface by Reaction Between Tetrameric Acid and Calcium Ion under Flow Condition and at the Batch Scale. *Industrial & Engineering Chemistry Research* **2019**, *58* (34), 15516-15525.
28. Nordgård, E. L.; Simon, S.; Sjöblom, J. Interfacial Shear Rheology of Calcium Naphthenate at the Oil/Water Interface and the Influence of pH, Calcium and in Presence of a Model Monoacid. *J. Dispersion Sci. Technol.* **2012**, *33* (7), 1083-1092.
29. Bertelli, J. N.; Dip, R. M. M.; Pires, R. V.; Albuquerque, F. C.; Lucas, E. F. Shear Rheology Using De Noüy Ring To Evaluate Formation and Inhibition of Calcium Naphthenate at the Water/Oil Interface. *Energy Fuels* **2014**, *28* (3), 1726-1735.
30. Simon, S.; Subramanian, S.; Gao, B.; Sjöblom, J. Interfacial Shear Rheology of Gels Formed at the Oil/Water Interface by Tetrameric Acid and Calcium Ion: Influence of Tetrameric Acid Structure and Oil Composition. *Ind. Eng. Chem. Res.* **2015**, *54* (35), 8713-8722.
31. Subramanian, S.; Simon, S.; Sjöblom, J. Interfacial dilational rheology properties of films formed at the oil/water interface by reaction between tetrameric acid and calcium ion. *J. Dispersion Sci. Technol.* **2017**, *38* (8), 1110-1116.
32. Simon, S.; Gao, B.; Tofte, S.; Sjöblom, J.; Passade-Boupat, N.; Palermo, T.; Rondon-Gonzalez, M. Influence of Asphaltenes on Gelation of Tetrameric Acid with Calcium Ion at the Oil/Water Interface under Flow-Model Condition. *Energy & Fuels* **2020**, *34* (5), 5846-5855.

33. Mediaas, H.; Grande, K. V.; Hustad, B. M.; Rasch, A.; Rueslåtten, H. G.; Vindstad, J. E. In *The Acid-IER Method - a Method for Selective Isolation of Carboxylic Acids from Crude Oils and Other Organic Solvents*, 5th International Symposium on Oilfield Scale, SPE 80404, Aberdeen, United Kingdom, January 29-30 2003.
34. Hannisdal, A.; Hemmingsen, P. V.; Sjöblom, J. Group-Type Analysis of Heavy Crude Oils Using Vibrational Spectroscopy in Combination with Multivariate Analysis. *Industrial & Engineering Chemistry Research* **2005**, *44* (5), 1349-1357.
35. Sauerer, B.; Stukan, M.; Buiting, J.; Abdallah, W.; Andersen, S. Dynamic Asphaltene-Stearic Acid Competition at the Oil–Water Interface. *Langmuir* **2018**, *34* (19), 5558-5573.
36. Zarkar, S.; Pauchard, V.; Farooq, U.; Couzis, A.; Banerjee, S. Interfacial Properties of Asphaltenes at Toluene–Water Interfaces. *Langmuir* **2015**, *31* (17), 4878-4886.
37. Pradilla, D.; Simon, S.; Sjöblom, J. Mixed interfaces of asphaltenes and model demulsifiers part I: Adsorption and desorption of single components. *Colloids and Surfaces A: Physicochemical and Engineering Aspects* **2015**, *466* (0), 45-56.
38. Eastoe, J.; Dalton, J. S. Dynamic surface tension and adsorption mechanisms of surfactants at the air–water interface. *Adv. Colloid Interface Sci.* **2000**, *85* (2–3), 103-144.
39. Chang, C.-H.; Franses, E. I. Adsorption dynamics of surfactants at the air/water interface: a critical review of mathematical models, data, and mechanisms. *Colloids Surf., A* **1995**, *100* (0), 1-45.
40. Bertheussen, A.; Simon, S.; Sjöblom, J. Equilibrium partitioning of naphthenic acids and bases and their consequences on interfacial properties. *Colloids and Surfaces A: Physicochemical and Engineering Aspects* **2017**, *529*, 45-56.
41. Bouriat, P.; El Kerri, N.; Graciaa, A.; Lachaise, J. Properties of a Two-Dimensional Asphaltene Network at the Water/Cyclohexane Interface Deduced from Dynamic Tensiometry. *Langmuir* **2004**, *20* (18), 7459-7464.
42. Dicharry, C.; Arla, D.; Sinquin, A.; Graciaa, A.; Bouriat, P. Stability of water/crude oil emulsions based on interfacial dilatational rheology. *Journal of Colloid and Interface Science* **2006**, *297* (2), 785-791.
43. Havre, T. E.; Sjöblom, J.; Vindstad, J. E. Oil/Water-Partitioning and Interfacial Behavior of Naphthenic Acids. *J. Dispersion Sci. Technol.* **2003**, *24* (6), 789 - 801.
44. Rudin, J.; Wasan, D. T. Mechanisms for lowering of interfacial tension in alkali/acidic oil systems: effect of added surfactant. *Industrial & Engineering Chemistry Research* **1992**, *31* (8), 1899-1906.
45. Passade-Boupat, N.; Gingras, J.-P.; Desplobins, C.; Zhou, H. Could the Asphaltene Solubility Class Index Be Used as the “Wax Appearance Temperature” of Asphaltenes? Illustration through the Study of the Polydispersity of PetroPhase 2017 Asphaltenes. *Energy & Fuels* **2018**, *32* (3), 2760-2768.
46. Groenzin, H.; Mullins, O. C. Asphaltene Molecular Size and Structure. *J. Phys. Chem. A* **1999**, *103* (50), 11237-11245.
47. Groenzin, H.; Mullins, O. C. Molecular Size and Structure of Asphaltenes from Various Sources. *Energy & Fuels* **2000**, *14* (3), 677-684.
48. Pradilla, D.; Simon, S.; Sjöblom, J. Mixed Interfaces of Asphaltenes and Model Demulsifiers, Part II: Study of Desorption Mechanisms at Liquid/Liquid Interfaces. *Energy Fuels* **2015**, *29* (9), 5507-5518.
49. Rane, J. P.; Pauchard, V.; Couzis, A.; Banerjee, S. Interfacial Rheology of Asphaltenes at Oil–Water Interfaces and Interpretation of the Equation of State. *Langmuir* **2013**, *29* (15), 4750-4759.
50. Jeribi, M.; Almir-Assad, B.; Langevin, D.; Hénaut, I.; Argillier, J. F. Adsorption Kinetics of Asphaltenes at Liquid Interfaces. *Journal of Colloid and Interface Science* **2002**, *256* (2), 268-272.

TOC graphic:

